

gon-14 Functions With Class B and Class C Synthetic Multivulva Genes to Control Larval Growth in *Caenorhabditis elegans*

Michael A. Chesney,* Ambrose R. Kidd III[†] and Judith Kimble*^{*,†,§,1}

*Department of Biochemistry, [†]Program in Cellular and Molecular Biology, [‡]Laboratory of Genetics and [§]Howard Hughes Medical Institute, University of Wisconsin, Madison, Wisconsin 53706-1544

Manuscript received July 28, 2005

Accepted for publication November 9, 2005

ABSTRACT

Previous work showed that *C. elegans gon-14* is required for gonadogenesis. Here we report that *gon-14* encodes a protein with similarity to LIN-15B, a class B synMuv protein. An extensive region of GON-14 contains blocks of sequence similarity to transposases of the hAT superfamily, but key residues are not conserved, suggesting a distant relationship. GON-14 also contains a putative THAP DNA-binding domain. A rescuing *gon-14::GON-14::VENUS* reporter is broadly expressed during development and localizes to the nucleus. Strong loss-of-function and predicted null *gon-14* alleles have pleiotropic defects, including multivulval (Muv) defects and temperature-sensitive larval arrest. Although the *gon-14* Muv defect is not enhanced by synMuv mutations, *gon-14* interacts genetically with class B and class C synMuv genes, including *lin-35/Rb*, *let-418/Mi-2β*, and *trr-1/TRRAP*. The *gon-14; synMuv* double mutants arrest as larvae when grown under conditions supporting development to adulthood for the respective single mutants. The *gon-14* larval arrest is suppressed by loss of *mes-2/E(Z)*, *mes-6/ESC*, or *mes-4*, which encodes a SET domain protein. Additionally, *gon-14* affects expression of *pgl-1* and *lag-2*, two genes regulated by the synMuv genes. We suggest that *gon-14* functions with class B and class C synMuv genes to promote larval growth, in part by antagonizing MES-2,3,6/ESC-E(z) and MES-4.

CHROMATIN structure can influence a broad range of biologically important processes, such as transcription, DNA replication, DNA damage repair, and homologous recombination. The structure of chromatin is modulated by post-translational modifications to the N-terminal tails of histones and by the activity of chromatin remodeling factors (reviewed in JENUWEIN and ALLIS 2001; BECKER and HÖRZ 2002). Although considerable progress has been made in identifying biochemical and genetic pathways that regulate chromatin structure, much remains unknown regarding how these pathways are utilized to control development.

Caenorhabditis elegans vulval development has emerged as a model for analyzing the chromatin regulation of specific cell fate decisions. Vulval development is positively regulated by an RTK/Ras signaling pathway and antagonized by the synthetic Multivulva (*synMuv*) genes, which encode homologs of transcriptional regulators and chromatin remodeling factors (reviewed in FAY and HAN 2000; LIPSICK 2004). The *synMuv* genes fall into at least three classes, A, B, and C, which act redundantly to control cell fate specification in six ectodermal blast cells called the vulval precursor cells (VPCs) (FERGUSON and HORVITZ 1989; CEOL and HORVITZ 2004). In wild-type animals, three VPCs are induced to the vulval fate,

while the three others assume a hypodermal fate (SULSTON and HORVITZ 1977). Single mutants of class A or class B *synMuv* genes typically exhibit normal VPC specification; however, in double mutants lacking one class A gene and one class B gene, all six VPCs adopt vulval fates, a defect called *synMuv* (HORVITZ and SULSTON 1980; FERGUSON and HORVITZ 1989). Class C *synMuv* genes function redundantly in VPC specification with both class A and class B genes (CEOL and HORVITZ 2004).

Most relevant to this work are the class B *synMuv* genes, some of which encode nematode homologs of components integral to the vertebrate E2F–retinoblastoma (E2F–Rb) and NuRD (*nucleosome remodeling and histone deacetylation*) complexes (reviewed in FAY and HAN 2000; LIPSICK 2004). Studies in various organisms indicate that the E2F–Rb complex represses transcription of E2F target genes and cell cycle progression, in part by recruiting chromatin-modifying proteins such as histone deacetylases (HDACs) (reviewed in FROLOV and DYSON 2004). Experiments with *Drosophila* embryos revealed that homologs of many class B *synMuv* proteins are physically associated in larger E2F- and Rb-containing complexes, known as *Drosophila* RBF, dE2F2, and dMyb-interacting proteins (dREAM) and Myb–*synMuvB* (Myb–MuvB); both complexes contain homologs of class B *synMuv* proteins LIN-35/Rb, EFL-1/E2F2, DPL-1/DP, LIN-9/Mip130/TWIT, LIN-37/Mip40, LIN-53/RbAp48, and LIN-54/Mip120, while the Myb–MuvB complex includes

¹Corresponding author: Department of Biochemistry, University of Wisconsin, 433 Babcock Dr., Madison, WI 53706-1544.
E-mail: jekimble@wisc.edu

the additional class B homologs HDA-1/RPD3/HDAC, LIN-61/L(3)MBT, and LIN-52/dLIN-52 (KORENJEK *et al.* 2004; LEWIS *et al.* 2004). Although a dREAM or Myb–MuvB-related complex has not yet been purified in *C. elegans*, its existence is predicted on the basis of the common phenotypes of the class B synMuv mutants. In addition, some class B synMuv genes encode homologs of components of the NuRD complex, a transcriptional repressor complex that contains both histone deacetylase and ATP-dependent chromatin remodeling activities (reviewed in BECKER and HÖRZ 2002); these include HDA-1 and LIN-53, as well as LET-418/Mi-2 β (LU and HORVITZ 1998; SOLARI and AHRINGER 2000; VON ZELEWSKY *et al.* 2000; THOMAS *et al.* 2003). Biochemically, *C. elegans* LET-418 and HDA-1 were co-immunoprecipitated with another class B protein, MEP-1, leading to the suggestion that these factors form an analogous *C. elegans* NuRD complex (UNHAITHAYA *et al.* 2002). Other class B synMuv proteins include homologs of chromatin-associated proteins (*e.g.*, HPL-2/HP1) and zinc finger proteins (*e.g.*, LIN-13, LIN-15B, LIN-36, and TAM-1) (CLARK *et al.* 1994; HUANG *et al.* 1994; HSIEH *et al.* 1999; THOMAS and HORVITZ 1999; MELÉNDEZ and GREENWALD 2000; COUTEAU *et al.* 2002; REDDY and VILLENEUVE 2004). The class C synMuv genes encode homologs of components of the Tip60/NuA4-like histone acetyltransferase complex, implicating an additional chromatin-remodeling complex in *C. elegans* vulval development (CEOL and HORVITZ 2004). Therefore, both class B and class C synMuv proteins are likely to function as transcriptional or chromatin regulators.

Although the synMuv genes were identified by their synthetic vulval effects, some are also required for viability, larval growth, or development of other tissues, such as the gonad and male mating structures (FERGUSON and HORVITZ 1985, 1989; LU and HORVITZ 1998; BEITEL *et al.* 2000; MELÉNDEZ and GREENWALD 2000; VON ZELEWSKY *et al.* 2000; CEOL and HORVITZ 2001; BELFIORE *et al.* 2002; DUFOURCQ *et al.* 2002; UNHAITHAYA *et al.* 2002; THOMAS *et al.* 2003; CEOL and HORVITZ 2004). In addition, some synMuv genes interact synthetically with genes that regulate the cell cycle, pharyngeal morphogenesis, gonadogenesis, or larval growth (BOXEM and VAN DEN HEUVEL 2001; FAY *et al.* 2002, 2003, 2004; BENDER *et al.* 2004a; CUI *et al.* 2004; CARDOSO *et al.* 2005). Therefore, the synMuv genes have been implicated in the developmental control of many tissues.

Another group of transcriptional regulators critical to this work are the genes encoding the MES-2/MES-3/MES-6 complex, and MES-4, all of which are required for germline viability in *C. elegans*. The *mes-2* and *mes-6* genes encode orthologs of Drosophila Polycomb group proteins Enhancer of Zeste [E(Z)] and Extra Sex Combs (ESC), respectively (HOLDEMAN *et al.* 1998; KORF *et al.* 1998). MES-2 and MES-6 associate with MES-3, a novel protein, to form the *C. elegans* analog of the Drosophila ESC-E(Z) and mammalian EED-EZH2 com-

plexes (PAULSEN *et al.* 1995; XU *et al.* 2001; CAO and ZHANG 2004). The MES-2,3,6/ESC-E(Z) complex has histone H3 Lysine27 (H3-K27) methyltransferase activity and represses transcription (BENDER *et al.* 2004b; CAO and ZHANG 2004). In *C. elegans*, the complex maintains repressive di- and trimethyl H3-K27 marks on the X chromosome in the adult germline and in early embryos (FONG *et al.* 2002; BENDER *et al.* 2004b) and spatially restricts expression of Hox genes in the soma (ROSS and ZARKOWER 2003). MES-4 is a SET domain protein that functions in a separate complex to promote germline viability; MES-4 localization is correlated with marks of active transcription and is excluded from the germline X chromosome by the MES-2,3,6/ESC-E(Z) complex (FONG *et al.* 2002). Importantly, disruption of the *mes-2,3,6/ESC-E(Z)* genes or of *mes-4* can suppress certain class B synMuv mutant phenotypes (UNHAITHAYA *et al.* 2002; WANG *et al.* 2005). One simple interpretation is that class B synMuv and MES activities act antagonistically to control transcription.

Here we describe the cloning and genetic analysis of *gon-14*, a gene identified in a genetic screen for mutations with early gonad defects (SIEGFRIED *et al.* 2004). We find that *gon-14* encodes a homolog of LIN-15B, which is a class B synMuv protein. Sequence analyses of GON-14 and other LIN-15B paralogs reveal several motifs suggestive of DNA regulation. We demonstrate that a rescuing GON-14 reporter protein is broadly expressed and localizes to the nucleus. The *gon-14* locus does not act synthetically with class A or class B synMuv genes to control vulval development, but it does interact with class B and class C synMuv genes to control larval growth. Like some synMuv mutants, *gon-14* mutant defects are suppressed by disrupting the *mes* genes. Furthermore, *gon-14* mutants have defects in gene expression that are typical of class B synMuv mutants. Taken together, our results suggest that *gon-14* functions in the nucleus to affect gene expression and likely acts in a *lin-35/Rb*- and *let-418/Mi-2 β* -related process.

MATERIALS AND METHODS

Nematode strains and maintenance: Animals were grown at 20° unless stated otherwise. All strains were derivative of Bristol strain N2 (BRENNER 1974). The following mutations were described previously (HODGKIN 1997 and references therein): *LG I: mes-3(bn35), dpy-5(e61), lin-35(n745), unc-13(e1091), xnp-1(tm678)* (BENDER *et al.* 2004a); *LG II: rrf-3(pk1426)* (SIMMER *et al.* 2002), *lin-38(n751), trr-1(n3630)* (CEOL and HORVITZ 2004); *LG III: lin-37(n758), lin-36(n766), lin-9(n112), mut-7(pk204)* (KETTING *et al.* 1999), *rde-4(ne301)* (TABARA *et al.* 1999); *LG IV: eri-1(mg366)* (KENNEDY *et al.* 2004); *LG V: tam-1(cc567)* (HSIEH *et al.* 1999), *let-418(ar114), dpy-11(e224), gon-14(q10, q12, q552, q631, q686)* (SIEGFRIED *et al.* 2004), *snb-1(js124)* (NONET *et al.* 1998), *mys-1(n4075)* (CEOL and HORVITZ 2004), *unc-42(e270), him-5(e1490), psa-1(ku355)* (CUI *et al.* 2004), *nDf32* (PARK and HORVITZ 1986); and *LG X: lin-15B(n744), lin-15A(n767)*. The following dominant

GFP balancer chromosomes were used: *mIn1[mIs14 dpy-10(e128)] II* (EDGLEY and RIDDLER 2001), *hT2[qIs48](I;III)* (MISKOWSKI *et al.* 2001), *nT1[qIs51](IV;V)* (SIEGFRIED *et al.* 2004), and *DnT1[qIs50](IV;V)* (BELFIORE *et al.* 2002). We also used the translocation *eT1(III;V)* (HODGKIN 1997) and molecular markers *qIs57 [lag-2::GFP, unc-119(+)] II* and *qIs56 [lag-2::GFP, unc-119(+)] V* (SIEGFRIED *et al.* 2004).

Molecular and sequence analyses of *gon-14*: *gon-14* maps to approximate position +0.1 on *LG V* (SIEGFRIED *et al.* 2004). We tested five cosmids (K04A8, EGAP9, ZK1055, F44C4, and T10H9) for rescue of *gon-14* sterility by standard methods (MELLO and FIRE 1995). Two partially overlapping cosmids (ZK1055 and F44C4) rescued *gon-14(q12)* to fertility; rescue was also obtained by germline transformation of a PCR fragment containing F44C4.4, the only predicted locus common to both rescuing cosmids. RNA interference (RNAi) directed against this locus phenocopied the morphological defects of *gon-14* mutants. To sequence the *gon-14* alleles, the *gon-14* open reading frame was PCR amplified from genomic DNA (Expand High Fidelity PCR System; Roche, Indianapolis), and three independent PCR products were sequenced for each allele.

Cell lineage and laser ablation: Cell lineages were examined by standard methods (SULSTON and HORVITZ 1977). We identified *gon-14* homozygotes by their lack of GFP fluorescence among progeny of *gon-14(q12)/nT1[qIs51]* heterozygotes. L1 divisions of the somatic gonad precursors, Z1 and Z4, and L3 divisions of P3.p–P8.p were followed at room temperature (22°–23.5°) in wild-type and *gon-14(q12)* hermaphrodites. In some animals, one germ cell precursor, Z2 or Z3, was ablated prior to analysis to reduce the number of cells in the gonad and facilitate identification of Z1 and Z4 descendants; this ablation does not affect the Z1/Z4 lineage in wild-type animals.

Laser ablations were done as described (BARGMANN and AVERY 1995), using a Micropoint Ablation Laser System (Photonics Instruments, Arlington, IL). Cell ablations were verified 1–8 hr postoperative, and their effect on development was assessed in adults.

RNAi: RNAi feeding was done essentially as described (FRASER *et al.* 2000). Briefly, L3 or early L4 larvae were transferred to an “RNAi plate” seeded with bacteria expressing a gene-specific dsRNA and maintained for 24–36 hr. Adults were then transferred to a fresh RNAi plate and allowed to lay progeny for a period of 2–14 hr before removal. F₁ progeny on the second plate were scored.

The vector used was pPD129.36 “L4440” (TIMMONS and FIRE 1998) unless noted otherwise. The inserts were derived from cDNA clones or from PCR products amplified from either genomic or cDNA templates as follows: *gon-14*, *BamHI/HindIII* fragment from cDNA clone pYK569F11 (provided by Y. Kohara); *lin-15B*, PCR product from genomic template, 5′ primer GCACCAGCTCCGAAACCTATCACA, 3′ primer CCGACAATTTCTCCGTCTTCGAG; *mes-2*, PCR product from genomic template, 5′ primer TGCTTAAAGGCCACTTCAATGCTA, 3′ primer TTTGTTTGGCCATAGACGGTAGAG; *lin-35*, PCR product from cDNA cloned into pLitmus28i, 5′ primer AAACGAGCAGCCGATGAGCCT, 3′ primer AGTGCCGTGCA TCAAGAACAC; and *lin-15A*, *SacI/PstI* fragment after PCR of cDNA template, 5′ primer AACGTTGATGCTATGCCAATG, 3′ primer CTGCGTTCTACAGTGTCTCTGC. For other RNAi experiments, bacterial clones containing L4440 with inserts from the desired genes were obtained from MRC Geneservice (KAMATH *et al.* 2003). In all cases, HT115 transformed with the “empty” L4440 vector, containing the multiple cloning site flanked by T7 sites, was used as a control.

Construction of double mutants: Double mutants containing *gon-14(q12)* and a class A or class B synMuv allele or an

RNAi-deficient allele were constructed by standard genetic crosses. To confirm presence of a class A synMuv allele, we used *lin-35* or *lin-15B* RNAi; to confirm presence of a class B synMuv allele, we used *lin-15A* RNAi. In control experiments, *gon-14* single mutants did not exhibit enhanced multivulva defects in these RNAi assays (see also RESULTS). For *gon-14(q12); lin-36(n766)* double mutants, the presence of *n766* was confirmed by an allele-specific *MaeII* restriction site. To confirm the presence of RNAi-deficient mutants (*i.e.*, *rde-4* or *mut-7*), we assayed for resistance to *pos-1* RNAi, which caused highly penetrant embryonic lethality in wild-type animals and in *gon-14* single mutants.

Scoring phenotypes: **VPC induction:** Induction of the VPCs, P3.p–P8.p, was scored in mid-to-late L4 stage larvae, essentially as described (MOGHAL and STERNBERG 2003). Each VPC was assigned a score of 1 if both daughters had divided, 0.5 if only one daughter had divided, or 0 if neither one had divided.

Larval arrest: Adults were identified by presence of embryos, by an everted vulva, or by adult alae. Worms were scored as arrested larvae if they failed to reach adulthood within a defined time interval after embryos were laid (1 week at 20° or 60–72 hr at 25°). Some additional *gon-14(q12)* homozygotes were examined after 8 days at 25°.

Construction of the *gon-14::GON-14::VENUS* transgene: The *gon-14* genomic region was PCR amplified from cosmid ZK1055 and cloned into pPD95.67 to make pJK1069, which includes the *gon-14* coding region plus 3.8 kb of 5′- and 1.5 kb of 3′-flanking sequences. Site-directed mutagenesis was used to introduce *AvrII* and *SphI* sites at the 3′ end of *gon-14a* just before the stop codon. The *venus* coding region was PCR amplified from pPD95.79–*venus* (a gift from Takeshi Ishihara), using 5′ and 3′ primers containing *AvrII* and *SphI* sites, respectively, and cloned into the *gon-14+AvrII/SphI* vector, in frame with *gon-14a*, to make pJK1077. The DNA sequence was confirmed, and the plasmid was injected into adult hermaphrodites by standard methods (MELLO and FIRE 1995). We generated numerous *gon-14::GON-14::VENUS* transgenic lines that rescued *gon-14(q12)* to fertility (details available upon request). The expression pattern and subcellular localization of the *GON-14::VENUS* fusion protein were similar in all lines. We generated the *gon-14::GON-14::VENUS* described here as follows: pJK1077 was linearized with *FspI* and mixed with *S. cerevisiae* genomic DNA (Novagen) that had been fragmented by sonication. A mixture of 6 ng/μl *gon-14::GON-14::VENUS* and 95 ng/μl *S. cerevisiae* DNA was injected into the germline of *gon-14(q686 ts)* adults maintained at permissive temperature (20°). F₁ progeny of injected animals were shifted to 25° as L2–L4 larvae to select for fertile F₂. One rescuing transgene was integrated by gamma irradiation to generate *qIs89*.

Immunohistochemistry: Mixed-stage worms were fixed using a modified Finney-Ruvkun protocol (FINNEY and RUVKUN 1990). Homozygous *gon-14(q12)* mutants were isolated as non-GFP worms from the strain *gon-14(q12)/nT1[qIs51]*, using a COPAS Biosort worm sorter (Union Biometrica, Somerville, MA). The primary antibody used was a rabbit polyclonal anti-PGL-1 (KAWASAKI *et al.* 1998), a gift from Susan Strome, and the secondary antibody was Cy3-conjugated anti-rabbit (Jackson ImmunoResearch, West Grove, PA). Worms were costained with DAPI.

Sequence analysis: Amino acid sequence alignments were constructed with MegAlign v5.53 (DNASTAR, Madison, WI) by using the Clustal W method (CHENNA *et al.* 2003) and further modified by inspection. In all alignments, amino acid similarity was scored using the Blosum62 scoring matrix (HENIKOFF and HENIKOFF 1992). The genomic sequence of a putative *C. remanei* GON-14 ortholog was identified by using the *C. elegans gon-14* genomic sequence in a BLAST search of the *C. remanei* sequence assembly database provided by the Washington University Genome Sequencing Center. One significant hit

was identified, corresponding to a region within contig 8.2. A predicted exon-intron structure was then constructed by inspection.

RESULTS

Molecular identification of the *gon-14* locus: We identified the *gon-14* locus, F44C4.4, by a combination of genetic mapping, germline transformation, and RNAi (see MATERIALS AND METHODS). We then sequenced the F44C4.4 coding region of five *gon-14* alleles and found a molecular lesion associated with each allele (Figure 1A). This locus has also been called *iri-1*, for inosine triphosphate (IP₃) receptor interacting (WALKER *et al.* 2004). Our analysis of *gon-14/iri-1* extends this earlier work, but does not investigate the interaction between GON-14/IRI-1 and the *C. elegans* IP₃ receptor, ITR-1. For simplicity, we refer to the locus as *gon-14*.

Two isoforms, *gon-14a* and *gon-14b*, have been identified by analysis of cDNAs (WS140; <http://www.wormbase.org>); these two isoforms differ in the splice donor site of intron 13 and generate alternate reading frames in the last exon (Figure 1A). RT-PCR analysis indicates that both isoforms are major transcripts (data not shown). The relative importance of the two transcripts is unknown. Putative *C. briggsae* and *C. remanei* *gon-14* orthologs contain sequences corresponding to the last exon of *gon-14a*, but do not have a recognizable *gon-14b* (data not shown). The *gon-14b* transcript was described previously (WALKER *et al.* 2004). For simplicity, we refer to both transcripts as *gon-14*, because our analyses focus on motifs in the common region. Using RT-PCR, we found that SL1 is *trans*-spliced to the *gon-14* transcript at an AUG 48 nucleotides upstream of the previously predicted start AUG (data not shown). This upstream AUG is likely to be the actual translational start site, because the N-terminal region is part of a motif conserved in *C. briggsae* and *C. remanei* orthologs (see below).

Sequence analysis of LIN-15B homology domain: The GON-14 protein possesses a large domain with homology to LIN-15B, a class B synMuv protein (Figure 1A; also see WALKER *et al.* 2004). Specifically, amino acids 251–723 of GON-14 align with amino acids 70–553 of LIN-15B (24% identity, 44% similarity); we refer to this region as the LIN-15B homology domain (Figure 1A, data not shown). A BLAST search using the GON-14 sequence revealed significant similarity to seven *C. elegans* predicted open reading frames, including LIN-15B and six uncharacterized proteins. The search also revealed similarity to six *C. briggsae* predicted open reading frames, including putative orthologs of GON-14 and LIN-15B. All of these homologs aligned to the LIN-15B homology domain (data not shown; also see WALKER *et al.* 2004). No other BLAST hits were statistically significant (*E*-value < 0.001).

Further analysis of the LIN-15B homology domain using the NCBI conserved domain database

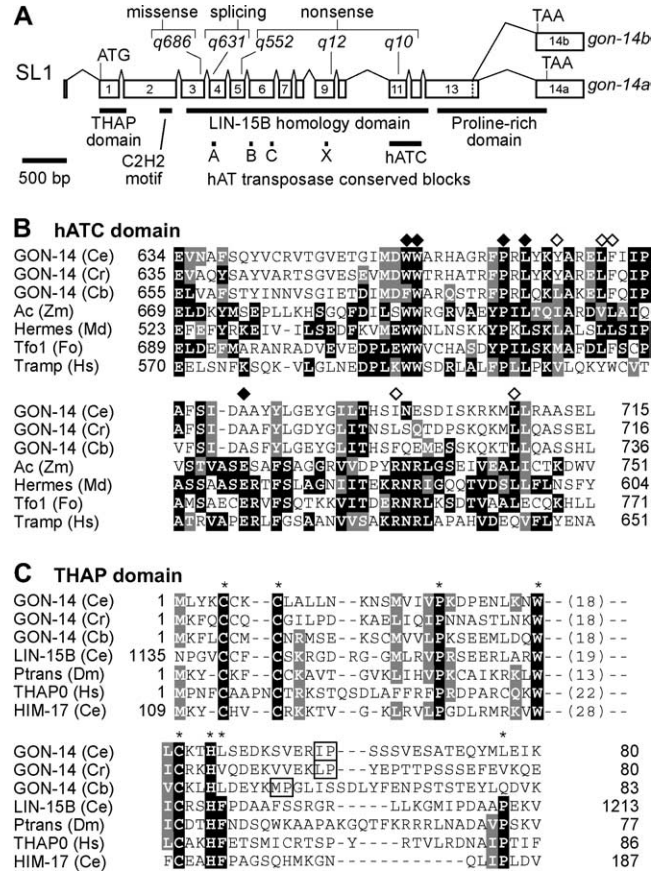


FIGURE 1.—The *gon-14* gene structure and predicted protein motifs. (A) *gon-14* gene structure, motifs, and mutations. The *gon-14* mRNA is *trans*-spliced to SL1. Two isoforms, *gon-14a* and *gon-14b*, differ in the splice donor site in exon 13, resulting in differing frame usage in exon 14; these are predicted to encode proteins of 923 and 883 amino acids, respectively. Locations of molecular lesions in *gon-14* alleles are indicated above the gene diagram; also see text. Solid bars below genes indicate motifs noted in the text. hAT transposase conserved blocks (A, B, C, and hATC) refer to regions typically conserved among hAT family proteins; the hATC domain contains blocks D, E, and F (RUBIN *et al.* 2001). Block X, an additional conserved region (this work). See also supplemental Figure 1 at <http://www.genetics.org/supplemental/>. Bar, 500 bp. (B) hATC domain: amino acid alignment of GON-14 orthologs to the hATC domains of representative hAT transposases. Ce, *C. elegans*; Cr, *C. remanei*; Cb, *C. briggsae*; Ac, Activator ORFa (*Zea mays*); Hermes (Md, *Musca domestica*); Tfo1 (Fo, *Fusarium oxysporum*); Tramp (Hs, *Homo sapiens*). Solid boxes, amino acid residues identical to at least two hAT transposases. Shaded boxes, residues similar to at least two identical or three similar hAT transposases. Similarity was scored on the basis of the Blosum62 matrix. Open diamond, residue important for dimerization and transposase activity in *Ac* and/or *Hermes* (ESSERS *et al.* 2000; MICHEL *et al.* 2003); solid diamond, residue important for transposase activity in *Ac* and/or *Hermes* (ESSERS *et al.* 2000; MICHEL *et al.* 2003; ZHOU *et al.* 2004). (C) THAP domain: alignment of THAP domains in GON-14 orthologs to THAP domains in related proteins. Ptrans, *Pelemont* transposase. Dm, *Drosophila melanogaster*. Other species abbreviations are as in Figure 1B. Asterisks, strictly conserved residues in THAP domains; solid boxes, identity to strictly conserved residues; shaded boxes, similarity to other conserved residues; boxed residues, potential similarity to the conserved proline (asterisk) and preceding small hydrophobic amino acid.

(MARCHLER-BAUER *et al.* 2003) revealed a motif with weak similarity to the hobo/Activator/Tam3 (hAT) transposase dimerization domain (hATC), pfam05699 (Figure 1, A and B). The hATC domain resides near the C terminus of DNA class II transposases of the hAT superfamily and is required for both *in vivo* transposase activity and *in vitro* dimerization (ESSERS *et al.* 2000; MICHEL *et al.* 2003). A multiple alignment of GON-14 to the hATC domains of representative hAT family proteins revealed conservation at several key residues required for hAT transposase activity and multimerization (Figure 1B; see also ESSERS *et al.* 2000; MICHEL *et al.* 2003). We next aligned the amino acid sequences of seven LIN-15B family members with representative hAT transposases and found additional regions of similarity outside the hATC domain; these regions corresponded to blocks of sequence that are typically conserved among hAT family members [Figure 1A (A, B, C, X); supplemental Figure 1 at <http://www.genetics.org/supplemental/>; RUBIN *et al.* 2001]. The conserved blocks are small (10–26 amino acids), but they span ~400 amino acids of the LIN-15B homology domain, and both order and approximate spacing of the blocks are conserved (supplemental Figure 1); the crystal structure of the *Hermes* hAT transposase revealed that blocks A, B, C, and hATC all contain residues situated in or near the active site (HICKMAN *et al.* 2005). However, the LIN-15B family proteins lack conservation at some key residues critical for transposase activity (Figure 1B; supplemental Figure 1).

Members of the hAT superfamily are mobile DNA elements (transposons) that each encode a transposase. The hAT transposase is necessary for catalyzing excision of the transposon from the genome and its reinsertion elsewhere in the genome (reviewed in KEMPKEN and WINDHOFER 2001). Signature features of hAT transposable elements include terminal inverted repeats (TIRs) that are typically 10–20 nucleotides in length, as well as 8-bp target site duplications flanking the insertion site. We analyzed the sequences flanking *lin-15B* family genes and did not detect TIRs or target site duplications (M. CHESNEY, unpublished observations). Notably, the *C. elegans* genome contains other genes that are putative hAT family members; these have both TIRs and target site duplications and encode proteins with stronger similarity to hAT transposases (BIGOT *et al.* 1996; RUBIN *et al.* 2001; M. CHESNEY, unpublished observations). We conclude that the *lin-15B* family encodes distant relatives of hAT transposases, but suggest that *lin-15B* family genes do not have typical hAT transposon/transposase behavior themselves.

Other motifs in the GON-14 sequence: To identify additional conserved motifs, we aligned the amino acid sequences of *C. elegans* GON-14 and the putative GON-14 orthologs from *C. briggsae* and *C. remanei*. *C. elegans* GON-14 is 44% identical and 60% similar to *C. briggsae* homolog CBG18977, and 46% identical and 66% sim-

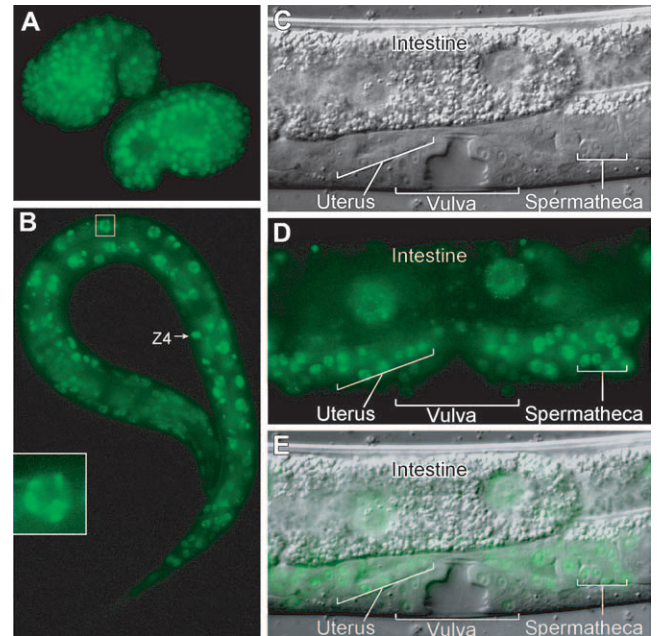


FIGURE 2.—GON-14::VENUS is broadly expressed and predominantly nuclear. (A) Comma stage embryos: GON-14::VENUS is present in most nuclei. (B) L1 larva: GON-14::VENUS is present in most nuclei. Inset, nucleus magnified; GON-14::VENUS localizes to nuclear speckles. (C–E) L4 larva. GON-14 is present in most nuclei, including the somatic gonad (anterior uterus and posterior spermatheca indicated), intestine, and vulva. GON-14::VENUS is concentrated in nuclear speckles and appears to be largely excluded from nucleoli. (C) Nomarski. (D) Fluorescence. (E) Merge.

ilar to *C. remanei* GON-14, along the full lengths of the respective proteins. These alignments revealed a C-X₂-C-X₄₁-C-X₂-H domain near the N terminus that resembles the *Thanatos-associated protein* (THAP) DNA-binding domain (Figure 1, A and C) (ROUSSIGNE *et al.* 2003); this motif was also identified in a recent database search for THAP domain-containing proteins (CLOUAIRE *et al.* 2005). The N-terminal location of the GON-14 THAP domain is typical of THAP-containing proteins, but the GON-14 THAP domain lacks key phenylalanine and proline residues and is therefore divergent (Figure 1C; see also CLOUAIRE *et al.* 2005). The GON-14 alignments also revealed a C-X₂-C-X₁₅-H-X₄-H (C2H2) motif just N-terminal to the LIN-15B homology domain. WALKER *et al.* (2004) noted a C-terminal proline-rich domain, which is also present in the *C. briggsae* and *C. remanei* orthologs (Figure 1A, data not shown).

GON-14 is a nuclear protein: To determine the pattern of *gon-14* expression and to learn the subcellular localization of GON-14 protein, we generated an integrated transgene, called *gon-14::GON-14::VENUS*, that rescued the defects of *gon-14* mutants (see MATERIALS AND METHODS). GON-14::VENUS was broadly expressed in somatic cells, beginning in ~50 cell embryos (data not shown). Expression persisted throughout embryogenesis (Figure 2A) and larval development (Figure 2,

B–E), but became fainter in adults (data not shown). Of particular note, GON-14::VENUS was present in the somatic gonadal precursors, Z1 and Z4, and the developing somatic gonad (Figure 2, B–E; supplemental Figure 2 at <http://www.genetics.org/supplemental/>; data not shown); the VPCs and developing vulva (Figure 2, C–E; supplemental Figure 2); and in the intestine (Figure 2, B–E; supplemental Figure 2). GON-14::VENUS was predominantly nuclear (Figure 2, A–E) and often concentrated in nuclear puncta or speckles (Figure 2, B (inset) and C–E). The number of speckles per nucleus varied from a few to >30 (Figure 2 and data not shown). We did not detect expression in the germline; however, we cannot exclude the possibility that this was a result of transgene silencing, as germline-expressed genes are often silenced when present on transgenes (KELLY *et al.* 1997).

Identification of a *gon-14* null allele: To assess *gon-14* function, we first identified a likely null mutant. Three *gon-14* alleles were the best candidates: *gon-14(q12)* and *gon-14(q10)* each contain G to A nucleotide changes that result in premature termination codons at amino acids 598 and 656, respectively, while *gon-14(q552)* contains a seven-nucleotide deletion that alters the reading frame from amino acid 398 and results in a premature termination codon. By contrast, *gon-14(q686)* contains a C to T nucleotide change that results in a missense mutation, P289S, and *gon-14(q631)* has a single nucleotide change (G to A) in the splice acceptor site of the third intron, which impairs splicing of this intron (data not shown). Phenotypic analysis supports the conclusion that *q10*, *q12*, and *q552* are all strong loss-of-function alleles and putative nulls. At 25°, *q10*, *q12*, and *q552* mutants were phenotypically indistinguishable: they arrested as midstage larvae (see below), while *q631* and *q686* homozygotes became sterile adults (SIEGFRIED *et al.* 2004 and this work). Furthermore, the *q12* phenotype was not enhanced when placed in *trans* to *nDf32*, a deficiency that removes the entire *gon-14* locus, but both *q631* and *q686* became more severe when placed in *trans* to *nDf32* (SIEGFRIED *et al.* 2004; data not shown). Therefore, all further characterization was conducted with *gon-14(q12)*, which is referred to as *gon-14(0)*.

***gon-14* is a pleiotropic regulator of animal development:** Previous studies reported pleiotropic defects of hypomorphic *gon-14* mutants (SIEGFRIED *et al.* 2004) or animals treated with *gon-14* RNAi (KAMATH *et al.* 2003; SIMMER *et al.* 2003; WALKER *et al.* 2004). Our analysis of *gon-14(0)* mutants confirms and extends these previous reports. The *gon-14(0)* mutant exhibited defects in growth, organogenesis, and cell division (see below). These defects were more severe at 25° (SIEGFRIED *et al.* 2004; this work), suggesting that removal of *gon-14* reveals a temperature-sensitive process.

Gonad defects: Wild-type adult hermaphrodites possess a gonad with two U-shaped gonadal arms and centrally

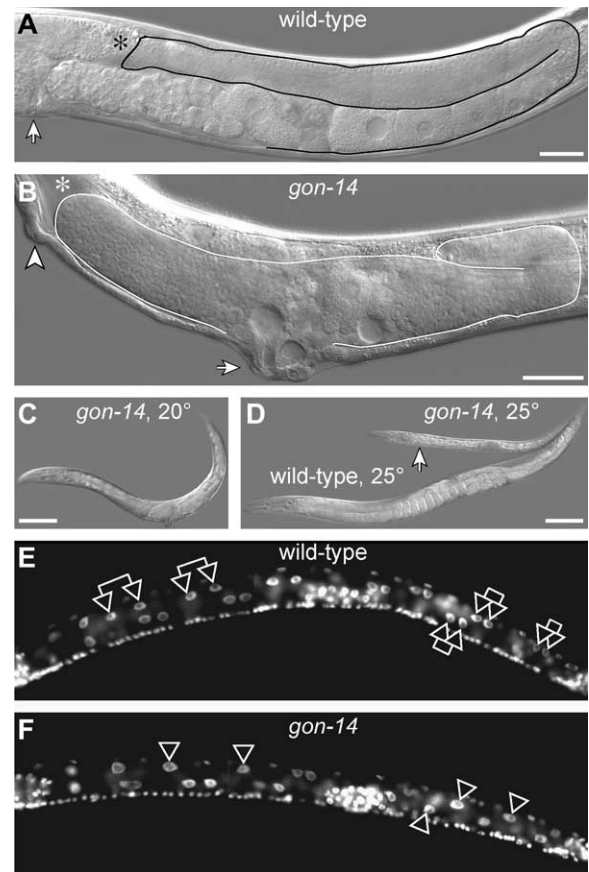


FIGURE 3.—Pleiotropic phenotype of *gon-14(0)* mutants. (A) Wild-type adult raised at 20°. Solid line, outline of posterior gonadal arm. Asterisk, distal end of gonadal arm is out of focal plane. Arrow, vulva. Bar, 25 μ m. (B) *gon-14(q12)* adult raised at 20°. Solid line, outline of malformed gonad. Asterisk, anterior gonad arm reflexed out of the focal plane. Arrow, protruding vulva. Arrowhead, ectopic pseudovulva. Bar, 25 μ m. (C) Size of *gon-14(q12)* mutant raised at 20°. Bar, 100 μ m. (D) Sizes of wild-type adult (bottom) and arrested *gon-14(q12)* mutant (arrow), both raised at 25°. Bar, 100 μ m. (E) Wild-type L2 raised at 25°. Double arrows, selected intestinal sister nuclei. (F) *gon-14(q12)* L2 or L3 raised at 25°, DAPI stained. Single arrowheads, single intestinal nuclei that have failed to divide.

located somatic gonadal structures that open into the vulva (Figure 3A). By contrast, *gon-14(0)* mutants grown at 20° developed into sterile adults that typically had short or abnormally shaped gonad arms and sometimes lacked one or both arms (Figure 3B, data not shown). The *gon-14* gonad often lacked a recognizable uterus or spermatheca, and the vulva was typically protruding (89%, $n = 126$). The incidence of loss of gonadal arms correlated with loss of expression of the *lag-2::GFP* distal tip cell marker, suggesting that in such cases either the distal tip cell was not made or its cell fate was not properly specified (data not shown). The *gon-14(0)* adult germline typically produced sperm (85%, $n = 33$) and abnormally shaped oocytes (91%, $n = 33$). Spermatocytes were also often observed in the body cavity, suggesting a defect in gonadal integrity. In some

cases, *gon-14(0)* adults produced one or more fertilized embryos (18%, $n = 33$) that appeared to arrest early in embryogenesis (<100 cells, data not shown).

Growth defects: When grown at 20°, *gon-14(0)* mutants reached adulthood ~12–24 hr later than wild-type animals, and mutant adults were typically smaller than wild type (compare *gon-14* worm in Figure 3C to wild-type worm in Figure 3D). When grown at 25°, mutants were about half as long as wild-type adults (Figure 3D), and after 1 week they usually showed no sign of vulval morphogenesis and did not make adult alae. Therefore, these *gon-14(0)* mutants appear to have arrested as midstage larvae. In addition, they were often constipated, consistent with previous reports of defecation defects (WALKER *et al.* 2004).

Cell division defects: The *gon-14(0)* mutants exhibited variably disrupted cell divisions in intestine, gonad, and vulva. Wild-type animals hatch with 20 intestinal nuclei, 14 of which divide during L1, to give rise to 34 intestinal nuclei by L2 (SULSTON and HORVITZ 1977). When grown at 25°, both wild-type and *gon-14(0)* L1s had 20 intestinal nuclei at hatching ($n = 10$); however, wild-type L2 larvae had 33 ± 1 nuclei ($n = 10$), whereas *gon-14(0)* L2s had only 24 ± 3 ($n = 28$) (Figure 3, E and F). In addition, somatic gonadal divisions were delayed in *gon-14(0)* mutants. In the wild type, the somatic gonad precursor cells (SGPs), Z1 and Z4, generated eight cells by L1 lethargus ($n = 3$), whereas in *gon-14(0)* mutants the SGPs either had not divided or had divided only once to generate only two to four cells by L1 lethargus ($n = 4$). Divisions of the VPCs were also variably delayed in *gon-14(0)* mutants grown at 25°. In some mutants, no VPC divisions were observed, whereas in others VPC divisions commenced 12–48 hr later than in the wild type. The delay in vulval development may have been related to the delay in gonadogenesis, as the extent of VPC divisions generally correlated with the size of the gonad in arrested larvae (data not shown).

Vulval defects: When *gon-14(0)* mutants were grown at 20°, many had one or more ectopic vulvae (52%, $n = 183$) (Figure 3B). The *gon-14* ectopic vulvae were smaller than those typically seen in synMuv class A; class B double mutants and often not visible in early adults. Ectopic vulvae were found in four different *gon-14* mutants (*q10*, *q12*, *q552*, and *q631*), but not when *gon-14* levels were reduced by RNAi in wild-type animals and only rarely when reduced by RNAi in *rxf-3*, an RNAi-hypersensitive mutant (data not shown). Therefore, *gon-14* mutants have a Muv defect.

Characterization of the *gon-14* Muv defect: The *gon-14* Muv defect was interesting in light of the molecular similarity between GON-14 and the LIN-15B synMuv protein. In wild-type animals, vulval fates are induced by signaling from the gonadal anchor cell, but in synMuv class A; class B double mutants, the VPCs can adopt vulval fates in the absence of the gonad (reviewed in FAY and HAN 2000). To learn whether *gon-14* ectopic vulvae

are dependent on the gonadal signal, we used laser microsurgery to eliminate all four cells of the gonadal primordium in *gon-14(0)* L1 larvae, thereby removing the entire gonad before the anchor cell was born. Control wild-type worms were vulvaless after this ablation ($n = 3$), but half of the gonad-ablated *gon-14(0)* mutants had ectopic vulvae ($n = 6$), a fraction similar to that typical of untreated *gon-14* mutants (see above). We conclude that the *gon-14* Muv defect is independent of the gonad inductive signal.

Next, we examined the origin of the ectopic vulvae in *gon-14(0)* mutants. In wild-type hermaphrodites, three VPCs, P5.p, P6.p, and P7.p, adopt vulval fates and undergo two to three rounds of divisions to generate 22 vulval cells; the uninduced VPCs, P3.p, P4.p, and P8.p, typically divide once each before fusing with the hypodermis (SULSTON and HORVITZ 1977). By contrast, in synMuv class A; class B double mutants, all six VPCs can adopt vulval fates, resulting in the formation of ectopic vulval protrusions (FERGUSON *et al.* 1987; FERGUSON and HORVITZ 1989). We examined the early VPC divisions of *gon-14(0)* and found that the daughters of P4.p and P8.p sometimes divided ectopically and their descendants failed to fuse with the hypodermis ($n = 2$). Consistent with these observations, examination of mid-L4 stage *gon-14(0)* larvae revealed frequent hyperproliferation of P3.p, P4.p, and P8.p (below and Table 1), indicating that *gon-14* controls VPC fate specification.

Is *gon-14* a synMuv gene? We next asked whether *gon-14* exhibits the synMuv defect. If *gon-14* functions as a class A or class B synMuv gene, the penetrance of *gon-14(0)* Muv animals should be enhanced by a synMuv class B or class A mutation, respectively. For most synMuv loci, a Muv defect occurs only when both a class A gene and a class B gene are disrupted (FERGUSON and HORVITZ 1989). However, for at least three class B synMuv loci, *hda-1*, *mep-1*, and *lin-13*, single mutants display a Muv phenotype under certain conditions: *hda-1* and *mep-1* are Muv at low penetrance as single mutants (BELFIORE *et al.* 2002; DUFOURCQ *et al.* 2002), but Muv at higher penetrance as double mutants that also remove a class A synMuv gene (UNHAVAITHAYA *et al.* 2002; THOMAS *et al.* 2003). In addition, *lin-13* homozygotes are Muv at 25°, but behave as class B synMuv mutants at 15° (MELÉNDEZ and GREENWALD 2000).

To assess whether *gon-14* is a synMuv gene, we compared the number of VPCs induced in *gon-14(0)* single mutants to that in animals carrying both *gon-14(0)* and either a class A or a class B synMuv mutation (Table 1). Wild-type animals grown at 20° had 3.0 induced VPCs ($n = 30$), and *gon-14(0)* mutants had an average of 3.8 induced VPCs ($n = 54$). The *gon-14* Muv defect was not enhanced in double mutants with *lin-15A* (class A), *lin-38* (class A), or *lin-36* (class B) synMuv mutations (Table 1). We conclude that *gon-14* is not a class A or a class B synMuv gene.

TABLE 1
gon-14* mutants exhibit multivulva defects but are not *synMuv

Genotype	% induction ^a						Average no. P(3–8).p vulval fates ± SE ^b	% animals with >3 vulval fates	<i>n</i>
	P3.p	P4.p	P5.p	P6.p	P7.p	P8.p			
Wild type	0	0	100	100	100	0	3.0 ± 0.0	0	30
<i>lin-15A</i> (n767)	0	1	100	100	100	0	3.0 ± 0.0	2	50
<i>lin-38</i> (n751)	0	0	100	100	100	0	3.0 ± 0.0	0	40
<i>lin-36</i> (n766)	0	0	100	100	100	0	3.0 ± 0.0	0	30
<i>lin-36</i> (n766); <i>lin-15A</i> (n767)	83	98	100	100	100	88	5.7 ± 0.1	100	30
<i>gon-14</i> (q12) ^c	17	23	96	100	100	40	3.8 ± 0.1	69	54
<i>gon-14</i> (q12); <i>lin-15A</i> (n767) ^c	11	18	100	100	100	28	3.6 ± 0.1	46	52
<i>lin-38</i> (n751); <i>gon-14</i> (q12) ^c	14	17	97	100	94	33	3.6 ± 0.1	52	33
<i>lin-36</i> (n766); <i>gon-14</i> (q12) ^c	17	22	98	98	98	42	3.8 ± 0.1	60	30

^a Percentage of animals in which the given VPC was induced (see MATERIALS AND METHODS).

^b Average number of P(3–8).p vulval fates per animal (see MATERIALS AND METHODS).

^c *gon-14* homozygotes were derived from heterozygous *gon-14* parents.

***gon-14* functions with class B and class C *synMuv* genes to control larval development:** While testing *gon-14* for *synMuv* activity (see above), we discovered a synthetic larval arrest defect in certain *gon-14*; *synMuv B* double mutants. Whereas *gon-14*(0) single mutants developed into adults at 20°, *gon-14*; *lin-15B* and *lin-35*; *gon-14* double mutants arrested as L1- or L2-sized larvae at the same temperature (Figure 4, B and C). The double mutants could undergo some postembryonic cell divisions in gonad, intestine, M, and P lineages, and in rare cases one or more VPCs divided; however, the arrested larvae never exhibited a mature vulva or adult alae (data not shown).

We explored whether other *synMuv* or *synMuv*-related genes exhibited similar interactions with *gon-14* by constructing additional double mutants or by using *gon-14* RNAi. Figure 4A summarizes the genes tested in this work and their protein products. In control experiments, we saw little or no larval arrest after *gon-14* RNAi of wild-type worms or of RNAi-hypersensitive mutants *rrf-3* or *eri-1* (Figure 4C). However, we observed highly penetrant larval arrest when testing *gon-14* RNAi of several class B *synMuv* mutants, including *lin-35*, *lin-15B*, *lin-9*, *lin-37*, and the class C mutant *trr-1*. In each of these cases, the *gon-14*(RNAi); *synMuv* defects were phenocopied by *gon-14*(0); *synMuv* double mutants (Figure 4C). We also observed highly penetrant larval arrest defects in *let-418 gon-14*(RNAi) animals, whereas less penetrant larval arrest defects were seen in *gon-14*(RNAi) *mys-1* animals, and little or no larval arrest was observed in *lin-36*; *gon-14* double mutants or in *lin-36*; *gon-14*(RNAi) or *tam-1 gon-14*(RNAi) animals (Figure 4C). Additionally, no larval arrest was observed when *gon-14* was disrupted in class A *synMuv* mutant backgrounds (data not shown). Therefore, *gon-14* interacts with many, but not all, *synMuv* genes to control larval growth.

The class B *synMuv* genes interact genetically with some Swi/Snf family members to promote larval growth,

including *psa-1*/SWI3 and *xnp-1*/ATR-X (BENDER *et al.* 2004a; CUI *et al.* 2004; CARDOSO *et al.* 2005). To ask whether *gon-14* also interacts with these genes, we tested *gon-14* RNAi in *psa-1* and *xnp-1* mutants. In both cases, *gon-14* RNAi caused highly penetrant larval arrest defects that were not observed in the single mutants (Figure 4C), indicating that *gon-14* functions redundantly with these Swi/Snf family genes to promote larval growth.

***gon-14* larval arrest is suppressed by disrupting the *mes* genes:** The larval arrest of two class B *synMuv* mutants, *mep-1* and *let-418*/Mi-2β, can be suppressed by disruption of *mes-2*, *mes-3*, *mes-4*, or *mes-6* (UNHAVAITHAYA *et al.* 2002), indicating that the *synMuv* genes antagonize the *mes-2,3,6*/ESC-E(Z) and *mes-4* genes in control of larval development. To determine whether *gon-14*(0) mutants share this property, we disrupted the *mes* genes by RNAi in *gon-14* mutants grown at 25°. All *gon-14*(0) mutants exhibited larval arrest in control experiments, but most developed into sterile adults when *mes-2*, *mes-3*, *mes-4*, or *mes-6* was depleted by RNAi (Figure 5, A and C). Although the *mes* genes are required for RNAi, previous studies have demonstrated the feasibility of using RNAi to knock down genes required for RNAi (DUDLEY *et al.* 2002; KIM *et al.* 2005). A similar, but less penetrant, suppression of larval arrest was seen in *mes-3*(bn35); *gon-14*(0) double mutants lacking maternal and zygotic wild-type *mes-3* (Figure 5C). Since the *mes* genes are required for RNAi (DUDLEY *et al.* 2002), we asked whether the *gon-14*(0) larval arrest could be suppressed by disrupting the RNAi pathway. However, *rde-4*; *gon-14* and *mut-7*; *gon-14* double mutants arrested as larvae at 25° (Figure 5C). Therefore, the suppression is not due to the disruption of RNAi.

We next asked whether *mes-2* or *mes-4* RNAi could suppress the larval arrest of *gon-14*; *synMuv B* double mutants. Indeed, both *mes-2* and *mes-4* RNAi partially suppressed the larval arrest defects of several *gon-14*; *synMuv B* double mutants (Figure 5, B and C). These

A Genes tested for synthetic interaction with *gon-14*

Gene name (synMuv class)	Homologs (motifs)	Putative complexes*
<i>lin-9</i> (B)	Mip130/Twit, Aly, hLin-9	dREAM, Myb-MuvB
<i>lin-15B</i> (B)	novel (THAP)	unknown
<i>lin-35</i> (B)	Rb, p107, p130	E2F/Rb, dREAM, Myb-MuvB
<i>lin-37</i> (B)	Mip40	dREAM, Myb-MuvB
<i>let-418</i> (B)	Mi-2β/CHD4	NuRD
<i>tam-1</i> (B)	novel (Ring finger, B-box)	unknown
<i>lin-36</i> (B)	novel (THAP)	unknown
<i>trr-1</i> (C)	TRRAP, Tra1p	Tip60/NuA4, STAGA, TFTC, PCAF, SAGA
<i>mys-1</i> (C)	Tip60, Esa1p	Tip60/NuA4
<i>xnp-1</i>	ATR-X, XNP, SNF2	ATR-X-Daxx
<i>psa-1</i>	SWI3	SWI/SNF, RSC, BRM, Brg1

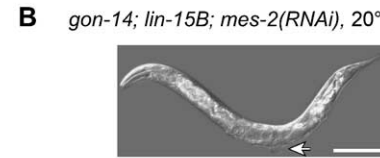
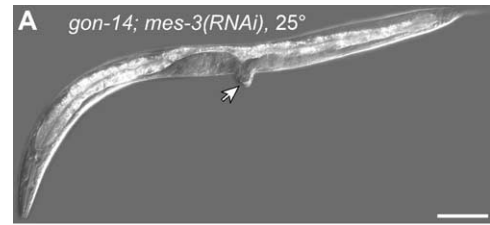
B

C Percent larval arrest at 20° (n)

gene-x	gene-x, +	gene-x, gon-14 RNAi	gene-x, gon-14(q12)**
+	0.0 (> 500)	0.0 (626)	3.9 (77)
<i>rff-3(pk1426)</i>	0.0 (70)	3.4 (87)	nd
<i>eri-1(mg366)</i>	0.0 (75)	0.0 (132)	nd
<i>lin-9(n112)</i>	0.0 (176)	100.0 (187)	100.0 (27)
<i>lin-15B(n744)</i>	0.0 (245)	100.0 (> 500)	100.0 (> 100)
<i>lin-35(n745)</i>	0.0 (172)	100.0 (> 500)	100.0 (> 100)
<i>lin-37(n758)</i>	0.4 (259)	100.0 (254)	100.0 (48)
<i>let-418(ar114)**</i>	3.8 (106)	93.0 (57)	nd
<i>tam-1(cc567)</i>	0.0 (518)	8.3 (495)	nd
<i>lin-36(n766)</i>	0.0 (547)	0.2 (520)	0.0 (22)
<i>trr-1(n3630)**</i>	0.0 (152)	99.3 (149)	100.0 (31)
<i>mys-1(n4075)**</i>	0.0 (52)	22.1 (86)	nd
<i>xnp-1(tm678)</i>	0.0 (74)	100.0 (67)	nd
<i>psa-1(ku355)</i>	0.0 (83)	91.4 (70)	nd

FIGURE 4.—*gon-14* interacts genetically with the class B and class C synMuv genes to control larval growth. (A) Genes tested for *gon-14* interactions, including members of the B and C synMuv classes as well as other genes that interact synthetically with the class B synMuv pathway. Asterisk, predicted protein complexes based on biochemical data from various organisms. See text for references. (B) *gon-14(q12)* single-mutant adult and *gon-14(q12); lin-15B(n744)* double-mutant arrested larva, both raised at 20°. Bar, 100 μm. (C) Frequency of larval arrest scored in *gene-X* single mutants, *gon-14* animals, and *gene-X; gon-14* animals, where *gene-X* is a synMuv mutant, a synMuv-interacting mutant, or an RNAi-hypersensitive mutant. *gon-14* was disrupted by RNAi or by using a putative null allele, *gon-14(q12)*, as noted. Double asterisk, progeny scored were descendants from parents heterozygous for the indicated allele. All were raised at 20°.

gon-14; synMuv B; mes(RNAi) animals were typically smaller than wild-type adults, but often had everted vulvae diagnostic of adulthood, whereas control *gon-14; synMuv B* double mutants did not reach adulthood (Figure 5, B and C). Furthermore, among animals that



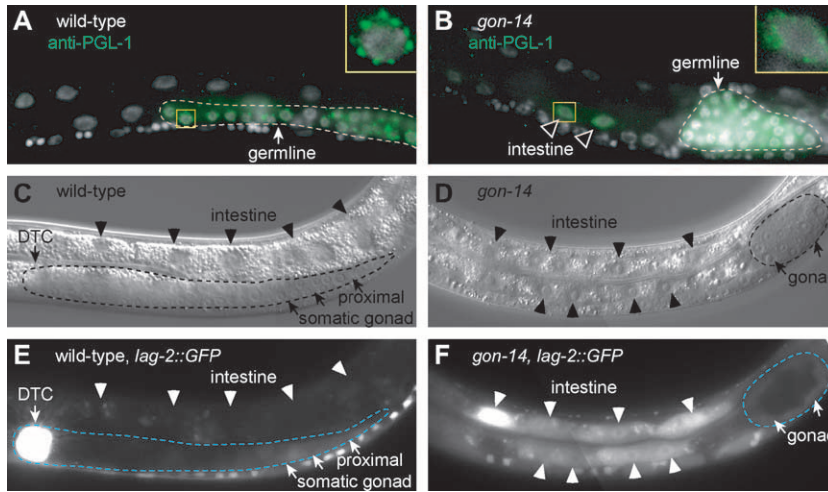
C Suppression of larval arrest by *mes* RNAi

Genotype	Temp. (°C)	% Adult progeny (n)
<i>gon-14(q12)</i>	25	0 (> 100)
<i>gon-14(q12); mes-2(RNAi)</i>	25	96 (25)
<i>gon-14(q12); mes-3(RNAi)</i>	25	100 (34)
<i>gon-14(q12); mes-3(bn35)</i>	25	50 (22)
<i>gon-14(q12); mes-4(RNAi)</i>	25	96 (26)
<i>gon-14(q12); mes-6(RNAi)</i>	25	100 (29)
<i>gon-14(q12); rde-4(ne301)</i>	25	0 (20)
<i>gon-14(q12); mut-7(pk204)</i>	25	0 (29)
<i>gon-14(q12)</i>	20	96 (77)
<i>gon-14(q12); lin-15B(n744)</i>	20	0 (> 100)
<i>gon-14(q12); lin-15B(n744); mes-2(RNAi)</i>	20	88 (33)
<i>gon-14(q12); lin-15B(n744); mes-4(RNAi)</i>	20	71 (21)
<i>gon-14(q12); lin-9(n112)</i>	20	0 (27)
<i>gon-14(q12); lin-9(n112); mes-2(RNAi)</i>	20	62 (42)
<i>gon-14(q12); lin-9(n112); mes-4(RNAi)</i>	20	90 (77)
<i>gon-14(q12); lin-37(n758)</i>	20	0 (48)
<i>gon-14(q12); lin-37(n758); mes-2(RNAi)</i>	20	13 (15)
<i>gon-14(q12); lin-37(n758); mes-4(RNAi)</i>	20	86 (65)
<i>gon-14(q12); lin-35(n745)</i>	20	0 (> 100)
<i>gon-14(q12); lin-35(n745); mes-2(RNAi)</i>	20	0 (37)
<i>gon-14(q12); lin-35(n745); mes-4(RNAi)</i>	20	0 (17)

FIGURE 5.—*gon-14* larval arrest is suppressed by *MES-2,3,6/ESC-E(Z)* or *MES-4* depletion. (A) *gon-14(q12); mes-3(RNAi)* reaches adulthood when grown at 25°. Arrow, protruding vulva. Bar, 100 μm. (B) *gon-14(q12); lin-15B(n744); mes-2(RNAi)* reaches adulthood when grown at 20°. Arrow, protruding vulva. Bar, 100 μm. (C) Percentage of adult progeny of the specified genotype. For clarity, gene names are not listed by map position.

failed to reach adulthood, those treated with *mes-2* or *mes-4* RNAi typically exhibited more cell proliferation in the gonad and vulva than control RNAi treated animals (data not shown), suggesting partial suppression in these cases. In general, *mes-4* RNAi caused more penetrant suppression of the *gon-14; synMuv B* larval arrest than did *mes-2* RNAi (Figure 5C). The reason for this disparity is unclear: in parallel experiments, both treatments caused highly penetrant sterility in *gon-14/+; synMuv B* animals (data not shown), indicating that the respective *mes* gene was knocked down in each case. We conclude that the *mes* genes are required for the *gon-14* single-mutant larval arrest at 25° and that both *mes-2* and *mes-4* promote the larval arrest of *gon-14; synMuv B* double mutants at 20°.

Altered gene expression in *gon-14* mutants: The class B synMuv genes also restrict the expression of certain



(E) Fluorescence. (D and F) Arrested *gon-14(0)* larva grown at 25°. *lag-2::GFP* is ectopically expressed in the intestine (arrowheads) and faintly expressed in the somatic gonad (arrows). The gonad is outlined by a dashed line. (D) Nomarski. (F) Fluorescence.

FIGURE 6.—*gon-14* represses PGL-1 and *lag-2::GFP* expression. (A) Wild-type L3 larva, stained with DAPI (white) and antibodies to PGL-1 (green). PGL-1 is restricted to germ cells, outlined by a dashed line. Inset, nucleus is shown; PGL-1 is localized in a punctate perinuclear pattern. (B) Arrested *gon-14(q12)* larva, stained with DAPI (white) and antibodies to PGL-1 (green). Ectopic PGL-1 is observed in intestinal nuclei (arrowheads). PGL-1 is also observed in germ cells, outlined by a dashed line. Inset, nucleus is shown; somatic PGL-1 is localized in a punctate perinuclear pattern. (C and E) Wild-type L3 grown at 25°. *lag-2::GFP* is expressed in the distal tip cell (DTC, arrow) and faintly in the proximal somatic gonad. The gonadal arm is outlined by a dashed line. *lag-2::GFP* is not expressed in the intestine (arrowheads). (C) Nomarski.

germline-specific factors, such as the P-granule-associated protein, PGL-1. Whereas PGL-1 is normally expressed only in the germline, several synMuv mutants ectopically express PGL-1 in somatic tissues (KAWASAKI *et al.* 1998; UNHAVAITHAYA *et al.* 2002; WANG *et al.* 2005). To learn whether *gon-14* shares this property, we examined PGL-1 protein in *gon-14(0)* mutants. PGL-1 was restricted to the germline in wild-type animals (Figure 6A), but it was observed ectopically in somatic cells of *gon-14(0)* mutants in addition to the normal germline staining (43%, $n = 54$) (Figure 6B). The effect was weaker than that reported for *mep-1* and *let-418*, as ectopic PGL-1 was generally visible in only a few somatic cells per mutant, typically in intestinal cells or hypodermal cells. The ectopic PGL-1 in *gon-14(0)* somatic cells was localized to perinuclear structures typical of PGL-1 in the P-granules of wild-type germ cells (Figure 6, A and B, insets). Therefore, *gon-14* affects PGL-1 expression.

In addition, most class B and class C synMuv genes repress expression of *lag-2*, such that loss of function results in ectopic *lag-2::GFP* reporter expression in the intestine and sometimes in the hypodermis (DUFOURCQ *et al.* 2002; POULIN *et al.* 2005). We similarly found that *lag-2::GFP* was ectopically expressed in *gon-14(0)* mutants. In wild-type larvae raised at 25°, *lag-2::GFP* was expressed in the gonadal primordium, ventral nerve cord, distal tip cells, vulva, and proximal gonad, but not in the intestine (Figure 6, C and E, and data not shown). By contrast, most *gon-14(0)* larvae raised at 25° exhibited ectopic *lag-2::GFP* expression in the intestine (Figure 6, D and F), indicating that *gon-14* antagonizes *lag-2* expression in the intestine.

DISCUSSION

In this work we describe the cloning and genetic characterization of *gon-14*, which encodes a homolog of

LIN-15B, a class B synMuv protein. Our work extends previous studies that characterized hypomorphic *gon-14* alleles or *gon-14/iri-1* RNAi (KAMATH *et al.* 2003; SIMMER *et al.* 2003; SIEGFRIED *et al.* 2004; WALKER *et al.* 2004) and supports three main conclusions. First, *gon-14* regulates gene expression, perhaps by chromatin regulation. Second, members of the LIN-15B protein family are distantly related to hAT transposases, and most also contain THAP motifs. On the basis of these findings and the similar roles of *gon-14* and *lin-15B*, we speculate that LIN-15B family members function in DNA regulation. Third, *gon-14* functions redundantly with *lin-35/Rb*, *let-418/Mi-2 β* , and other synMuv and synMuv-related genes, to promote larval growth and antagonize the *mes-2*, *3,6/ESC-E(Z)* and *mes-4* genes.

***gon-14* regulates gene expression:** Several lines of evidence suggest that *gon-14* affects gene expression, perhaps by chromatin regulation. First, loss of *gon-14* causes derepression of *lag-2* in the intestine and of *pgl-1* in somatic tissues. The class B synMuv genes, which are implicated in transcriptional repression and chromatin remodeling, are similarly required for repression of *lag-2* in the intestine and of *pgl-1* in the soma (DUFOURCQ *et al.* 2002; UNHAVAITHAYA *et al.* 2002; POULIN *et al.* 2005; WANG *et al.* 2005). A regulatory role for *gon-14* is further supported by the presence of two putative DNA binding motifs, THAP and C2H2, in the GON-14 sequence and by the nuclear localization of a rescuing GON-14::VENUS fusion protein. In addition, GON-14 interacts genetically with various genes that control transcription and chromatin, including *lin-35/Rb*, *let-418/Mi-2 β* , *trr-1/TRRAP*, *xnp-1/ATR-X*, *psa-1/SWI3*, and *mes-2/E(z)*. Furthermore, loss-of-function mutations in the genes encoding the POP-1/TCF and SYS-1/ β -catenin transcription factors are dominant enhancers of *gon-14* homozygotes (SIEGFRIED *et al.* 2004; KIDD *et al.* 2005). Therefore, GON-14 may establish a chromatin state critical for transcriptional activation by POP-1/TCF and SYS-1/ β -catenin.

The *gon-14* locus was previously implicated in signaling by the inosine triphosphate receptor, ITR-1 (WALKER *et al.* 2004). GON-14/IRI-1 and ITR-1 fragments interacted in yeast two-hybrid and *in vitro* binding assays. Furthermore, depletion of *gon-14/iri-1* by RNAi generated defects similar to those of *itr-1* mutants and enhanced a hypomorphic *itr-1* allele (WALKER *et al.* 2004). These findings led to the suggestion that GON-14/IRI-1 interacts with ITR-1 *in vivo* to modulate its function (WALKER *et al.* 2004). Our results suggest an alternative hypothesis, namely that *gon-14* affects ITR-1-regulated processes by affecting gene expression. However, these two hypotheses are not mutually exclusive.

The LIN-15B family: The LIN-15B protein family is defined by an ~470-amino-acid LIN-15B homology domain that exhibits similarity to hAT family transposases. The most prominent conserved feature is the hATC domain, but four additional blocks of residues are also conserved with hAT transposases; these blocks span ~400 amino acids of the LIN-15B homology domain, and both order and relative spacing of the blocks are conserved (this work; RUBIN *et al.* 2001). The functional significance of this sequence similarity is unknown. Some residues critical for transposition are not conserved, and our analysis does not support the classification of *lin-15B* family genes as likely hAT transposons. Perhaps the LIN-15B family has retained some properties of hAT transposases, such as multimerization or DNA binding, but deploys them for chromatin regulation rather than for transposition.

Recent work suggests that gene regulation by hAT transposase-like proteins is a mechanism employed in diverse phyla to control development. An Arabidopsis hAT transposase-like protein, DAYSLEEPER, was found to be essential for plant development and to regulate global gene expression. Like GON-14, DAYSLEEPER lacks some conserved residues, and the locus is not flanked by TIRs and 8-bp target site duplications (BUNDOCK and HOOYKAAS 2005). Thus, in at least two organisms, hAT-transposase-like proteins regulate gene expression and are required for development.

In addition to the LIN-15B homology domain, four *C. elegans* LIN-15B paralogs contain one or more THAP motifs (REDDY and VILLENEUVE 2004; CLOUAIRE *et al.* 2005; this work; M. CHESNEY, unpublished data). The THAP motifs of human THAP1 and Drosophila *P*-element transposase exhibit sequence-specific DNA-binding activity *in vitro* (LEE *et al.* 1998; CLOUAIRE *et al.* 2005). Therefore, GON-14 and its LIN-15B paralogs may bind to DNA. In addition, several THAP domain proteins have been implicated in chromatin regulation or DNA-associated functions. For instance, human THAP7 can recruit histone deacetylase to target sites (MACFARLAN *et al.* 2005). THAP domains are also present in two other synMuv proteins, LIN-36 and LIN-15A, as well as in HIM-17, a chromatin-associated protein required for initiation of meiotic recombina-

tion (REDDY and VILLENEUVE 2004). The GON-14 THAP domain is divergent (CLOUAIRE *et al.* 2005) and has not been tested for DNA-binding activity; however, this motif is conserved in putative orthologs from other nematodes, suggesting that it contributes to GON-14 function. The presence of THAP- and hAT-related domains in LIN-15B family proteins, together with the roles of both LIN-15B and GON-14 in gene expression (see above), suggests that LIN-15B family proteins have a common function in DNA regulation.

Redundancy between *gon-14* and *lin-15B*: Given the sequence similarity between GON-14 and LIN-15B, one prediction is that these proteins can substitute for each other to control processes critical for growth. Indeed, *gon-14; lin-15B* double mutants exhibit a synthetic early larval arrest. Although larval arrest can occur in *gon-14* single mutants grown at 25°, this larval arrest occurs later than that seen in *gon-14; lin-15B* double mutants. Therefore, GON-14 and LIN-15B may be interchangeable for larval growth. Alternatively, GON-14 and LIN-15B may act in distinct complexes with partially redundant functions. This latter idea is suggested by the fact that *lin-15B* and *gon-14* single mutants have different phenotypes: *lin-15B* mutants have no apparent defects on their own, while *gon-14* mutants have severe pleiotropic defects, including larval arrest at restrictive temperatures and sterility at all temperatures; moreover, *lin-15B* is a synMuv gene, but *gon-14* is not (FERGUSON and HORVITZ 1989; CLARK *et al.* 1994; HUANG *et al.* 1994; SIEGFRIED *et al.* 2004; this work). These differences are not a consequence of differential expression, as both GON-14 and LIN-15B are nuclear proteins and broadly expressed throughout development (this work; L. HUANG and P. STERNBERG, personal communication). Therefore, the individual functions of GON-14 and LIN-15B have clearly become specialized within the same cell. Consistent with this idea, the two proteins differ in domain architecture outside of the LIN-15B homology domain. For instance, GON-14 harbors a C2H2 motif just N-terminal to its LIN-15B homology domain, but LIN-15B lacks this motif. In addition, GON-14 has one N-terminal THAP domain, whereas LIN-15B has two C-terminal THAP domains (this work; REDDY and VILLENEUVE 2004; CLOUAIRE *et al.* 2005). These sequence differences may contribute to the distinct developmental roles of GON-14 and LIN-15B.

***gon-14* functions with the synMuv genes and antagonizes the *mes* genes to promote larval growth:** The *gon-14* locus is conditionally required for larval growth, and the larval growth defects are enhanced by mutations in several class B synMuv genes that encode homologs of components of the Rb and NuRD complexes. Additional enhancers include the class C genes *mys-1/Tip60* and *trr-1/TRRAP*, whose homologs are components of the Tip60/NuA4 histone acetyltransferase complex; TRRAP is also found in a variety of chromatin-remodeling complexes (TIMMERS and TORA 2005). The *gon-14* larval

arrest is similarly enhanced by mutations in the Swi/Snf family members *xnp-1*/ATR-X and *psa-1*/SWI3, whose homologs are also implicated in chromatin remodeling (MARTENS and WINSTON 2003; XUE *et al.* 2003). Therefore, *gon-14* genetically interacts with a variety of transcriptional regulators and chromatin remodeling factors in control of larval growth.

Further genetic analyses revealed that *gon-14* mutants share several defects in common with certain class B synMuv mutants, most notably those affecting the putative *C. elegans* NuRD (CeNuRD) components LET-418/Mi-2 β and MEP-1. Like both *let-418* and *mep-1*, the *gon-14* locus is essential for growth under certain conditions. The *gon-14* single mutant exhibits temperature-dependent larval arrest defects, while *let-418* and *mep-1* mutants arrest as larvae when both maternal and zygotic gene products are eliminated but develop into adults when a functional maternal copy is present (VON ZELEWSKY *et al.* 2000; BELFIORE *et al.* 2002; UNHAVAITHAYA *et al.* 2002; this work). In addition, the larval arrest defects of *gon-14*, *let-418*, and *mep-1* single mutants are suppressed by maternal and zygotic loss of the *mes-2,3,6*/ESC-E(Z) or *mes-4* genes (this work; UNHAVAITHAYA *et al.* 2002). Thus, both GON-14 and CeNuRD function antagonistically with MES-2,3,6/ESC-E(Z) and MES-4 in control of larval growth. Other phenotypic similarities between *gon-14*, *let-418*, and *mep-1* single mutants include sterility and gonadal and vulval morphological defects. (this work; VON ZELEWSKY *et al.* 2000; BELFIORE *et al.* 2002). In addition, like the CeNuRD components and most other class B synMuv genes, *gon-14* negatively regulates *lag-2* expression and represses somatic expression of PGL-1, a germline-specific protein (this work; DUFOURCQ *et al.* 2002; UNHAVAITHAYA *et al.* 2002; POULIN *et al.* 2005; WANG *et al.* 2005). On the basis of these observations and of the genetic interaction between *gon-14* and *let-418*/Mi-2 β , we propose that *gon-14* and CeNuRD function in a common process to promote larval growth.

The causes of the *gon-14* and *synMuv* mutant larval arrest defects are unknown, but genetic analyses of *gon-14*, CeNuRD components *let-418* and *mep-1*, and other class B synMuv genes have provided insights regarding a possible mechanism. One intriguing model is based on the apparently antagonistic activities of CeNuRD and the MES-2,3,6/ESC-E(Z) and MES-4 complexes. This model posits that the CeNuRD complex promotes a chromatin state that allows somatic developmental programs; in the absence of CeNuRD, the MES-2,3,6/ESC-E(Z) and MES-4 complexes promote a distinct chromatin state in somatic tissues that is typical of the germline and that partially represses somatic developmental programs (see SHIN and MELLO 2003; WANG *et al.* 2005). We propose that *gon-14* functions in a common process with CeNuRD components and other synMuv B genes to promote somatic developmental programs. In support of this model, loss of *gon-14*, *let-418*/Mi-2 β , or *mep-1*

causes ectopic expression in somatic tissues of germ cell-specific proteins, such as PGL-1, suggesting that the mutant soma has adopted a germ cell-like state (this work; UNHAVAITHAYA *et al.* 2002). Furthermore, disruption of the *mes* genes suppresses the larval arrest defects of *gon-14*, *let-418*, or *mep-1* single mutants and of *gon-14*; *synMuv B* double mutants and also partially suppresses the ectopic PGL-1 expression in *mep-1* mutants (this work; UNHAVAITHAYA *et al.* 2002). In the wild-type germline, the MES-2,3,6/ESC-E(Z) complex confers a repressive chromatin state on the X chromosome, while MES-4 binds to autosomes and colocalizes with marks of transcriptional activation (FONG *et al.* 2002; BENDER *et al.* 2004b). In the absence of CeNuRD or GON-14 activities, the MES-2,3,6/ESC-E(Z) and MES-4 complexes might disrupt somatic development by suppressing the somatic X chromosome or other sites important for somatic development and promoting the expression of germline-specific factors that inhibit somatic development.

The authors thank Susan Strome, Andy Fire, Takeshi Ishihara, and Josh Kaplan for antibodies, strains, and reporter constructs. Additional strains were provided by the *Caenorhabditis* Genetics Center. We thank members of the Kimble lab for helpful discussions and Maureen Barr and Tristana von Will for critical reading of the manuscript. We are also grateful to Peggy Kroll-Conner and Jadwiga Forster for technical assistance and to Anne Helsley-Marchbanks and Laura Vanderploeg for assistance in preparation of the manuscript and figures. M.A.C. and A.R.K. were supported by National Institutes of Health (NIH) predoctoral training grants, T32 GM08349 (biotechnology) and T32 GM07215 (molecular biosciences), respectively. J.K. is an investigator with the Howard Hughes Medical Institute. This work was supported by NIH grant GM069454 to J.K.

LITERATURE CITED

- BARGMANN, C. I., and L. AVERY, 1995 Laser killing of cells in *Caenorhabditis elegans*, pp. 225–250 in *Caenorhabditis elegans: Modern Biological Analysis of an Organism*, edited by H. F. EPSTEIN and D. C. SHAKES. Academic Press, San Diego.
- BECKER, P. B., and W. HÖRZ, 2002 ATP-dependent nucleosome remodeling. *Annu. Rev. Biochem.* **71**: 247–273.
- BEITEL, G. J., E. J. LAMBIE and H. R. HORVITZ, 2000 The *C. elegans* gene *lin-9*, which acts in an Rb-related pathway, is required for gonadal sheath cell development and encodes a novel protein. *Gene* **254**: 253–263.
- BELFIORE, M., L. D. MATHIES, P. PUGNALE, G. MOULDER, R. BARSTEAD *et al.*, 2002 The MEP-1 zinc-finger protein acts with MOG/DEAH box proteins to control gene expression via the *fem-3* 3' untranslated region in *Caenorhabditis elegans*. *RNA* **8**: 725–739.
- BENDER, A. M., O. WELLS and D. S. FAY, 2004a *lin-35*/Rb and *xnp-1*/ATR-X function redundantly to control somatic gonad development in *C. elegans*. *Dev. Biol.* **273**: 335–349.
- BENDER, L. B., R. CAO, Y. ZHANG and S. STROME, 2004b The MES-2/MES-3/MES-6 complex and regulation of histone H3 methylation in *C. elegans*. *Curr. Biol.* **14**: 1639–1643.
- BIGOT, Y., C. AUJE-GOUILLOU and G. PERIQUET, 1996 Computer analyses reveal a *hobo*-like element in the nematode *Caenorhabditis elegans*, which presents a conserved transposase domain common with the Tc1-Mariner transposon family. *Gene* **174**: 265–271.
- BOXEM, M., and S. VAN DEN HEUVEL, 2001 *lin-35* Rb and *cki-1* Cip/Kip cooperate in developmental regulation of G1 progression in *C. elegans*. *Development* **128**: 4349–4359.
- BRENNER, S., 1974 The genetics of *Caenorhabditis elegans*. *Genetics* **77**: 71–94.
- BUNDOCK, P., and P. HOOYKAAS, 2005 An *Arabidopsis* hAT-like transposase is essential for plant development. *Nature* **436**: 282–284.

- CAO, R., and Y. ZHANG, 2004 The functions of E(Z)/EZH2-mediated methylation of lysine 27 in histone H3. *Curr. Opin. Genet. Dev.* **14**: 155–164.
- CARDOSO, C., C. COUILLAUD, C. MIGNON-RAVIX, A. MILLET, J. J. EWBANK *et al.*, 2005 XNP-1/ATR-X acts with RB, HP1 and the NuRD complex during larval development in *C. elegans*. *Dev. Biol.* **278**: 49–59.
- CEOL, C. J., and H. R. HORVITZ, 2001 *dpl-1* DP and *eft-1* E2F act with *lin-35* Rb to antagonize Ras signaling in *C. elegans* vulval development. *Mol. Cell* **7**: 461–473.
- CEOL, C. J., and H. R. HORVITZ, 2004 A new class of *C. elegans* synMuv genes implicates a Tip60/NuA4-like HAT complex as a negative regulator of Ras signaling. *Dev. Cell* **6**: 563–576.
- CHENNA, R., H. SUGAWARA, T. KOIKE, R. LOPEZ, T. J. GIBSON *et al.*, 2003 Multiple sequence alignment with the Clustal series of programs. *Nucleic Acids Res.* **31**: 3497–3500.
- CLARK, S. G., X. LU and H. R. HORVITZ, 1994 The *Caenorhabditis elegans* locus *lin-15*, a negative regulator of a tyrosine kinase signaling pathway, encodes two different proteins. *Genetics* **137**: 987–997.
- CLOUAIRE, T., M. ROUSSIGNE, V. ECOCHARD, C. MATHE, F. AMALRIC *et al.*, 2005 The THAP domain of THAP1 is a large C2GH module with zinc-dependent sequence-specific DNA-binding activity. *Proc. Natl. Acad. Sci. USA* **102**: 6907–6912.
- COUTEAU, F., F. GUERRY, F. MULLER and F. PALLADINO, 2002 A heterochromatin protein 1 homologue in *Caenorhabditis elegans* acts in germline and vulval development. *EMBO Rep.* **3**: 235–241.
- CUI, M., D. S. FAY and M. HAN, 2004 *lin-35/Rb* cooperates with the SWI/SNF complex to control *Caenorhabditis elegans* larval development. *Genetics* **167**: 1177–1185.
- DUDLEY, N. R., J.-C. LABBÉ and B. GOLDSTEIN, 2002 Using RNA interference to identify genes required for RNA interference. *Proc. Natl. Acad. Sci. USA* **99**: 4191–4196.
- DUFOURCQ, P., M. VICTOR, F. GAY, D. CALVO, J. HODGKIN *et al.*, 2002 Functional requirement for histone deacetylase 1 in *Caenorhabditis elegans* gonadogenesis. *Mol. Cell Biol.* **22**: 3024–3034.
- EDGLEY, M. L., and D. L. RIDDLE, 2001 LG II balancer chromosomes in *Caenorhabditis elegans*. *mT1(II/III)* and the *mIn1* set of dominantly and recessively marked inversions. *Mol. Genet. Genomics* **266**: 385–395.
- ESSERS, L., R. H. ADOLPHS and R. KUNZE, 2000 A highly conserved domain of the maize *Activator* transposase is involved in dimerization. *Plant Cell* **12**: 211–224.
- FAY, D. S., and M. HAN, 2000 The synthetic multivulval genes of *C. elegans*: functional redundancy, Ras-antagonism, and cell fate determination. *Genesis* **26**: 279–284.
- FAY, D. S., S. KEENAN and M. HAN, 2002 *fwr-1* and *lin-35/Rb* function redundantly to control cell proliferation in *C. elegans* as revealed by a nonbiased synthetic screen. *Genes Dev.* **16**: 503–517.
- FAY, D. S., E. LARGE, M. HAN and M. DARLAND, 2003 *lin-35/Rb* and *ubc-18*, an E2 ubiquitin-conjugating enzyme, function redundantly to control pharyngeal morphogenesis in *C. elegans*. *Development* **130**: 3319–3330.
- FAY, D. S., X. QIU, E. LARGE, C. P. SMITH, S. MANGO *et al.*, 2004 The coordinate regulation of pharyngeal development in *C. elegans* by *lin-35/Rb*, *pha-1*, and *ubc-18*. *Dev. Biol.* **271**: 11–25.
- FERGUSON, E. L., and H. R. HORVITZ, 1985 Identification and characterization of 22 genes that affect the vulval cell lineages of *Caenorhabditis elegans*. *Genetics* **110**: 17–72.
- FERGUSON, E. L., and H. R. HORVITZ, 1989 The multivulva phenotype of certain *Caenorhabditis elegans* mutants results from defects in two functionally redundant pathways. *Genetics* **123**: 109–121.
- FERGUSON, E. L., P. W. STERNBERG and H. R. HORVITZ, 1987 A genetic pathway for the specification of the vulval cell lineages of *Caenorhabditis elegans*. *Nature* **326**: 259–267. (erratum: *Nature* **327**: 82).
- FINNEY, M., and G. RUVKUN, 1990 The *unc-86* gene product couples cell lineage and cell identity in *C. elegans*. *Cell* **63**: 895–905.
- FONG, Y., L. BENDER, W. WANG and S. STROME, 2002 Regulation of the different chromatin states of autosomes and X chromosomes in the germ line of *C. elegans*. *Science* **296**: 2235–2238.
- FRASER, A. G., R. S. KAMATH, P. ZIPPERLEN, M. MARTINEZ-CAMPOS, M. SOHRMANN *et al.*, 2000 Functional genomic analysis of *C. elegans* chromosome I by systematic RNA interference. *Nature* **408**: 325–330.
- FROLOV, M. V., and N. J. DYSON, 2004 Molecular mechanisms of E2F-dependent activation and pRB-mediated repression. *J. Cell Sci.* **117**: 2173–2181.
- HENIKOFF, S., and J. G. HENIKOFF, 1992 Amino acid substitution matrices from protein blocks. *Proc. Natl. Acad. Sci. USA* **89**: 10915–10919.
- HICKMAN, A. B., Z. N. PEREZ, L. ZHOU, P. MUSINGARIMI, R. GHIRLANDO *et al.*, 2005 Molecular architecture of a eukaryotic DNA topoisomerase. *Nat. Struct. Mol. Biol.* **12**: 715–721.
- HODGKIN, J., 1997 Appendix 1: Genetics, pp. 881–1047 in *C. elegans II*, edited by D. L. RIDDLE, T. BLUMENTHAL, B. J. MEYER and J. R. PRIESS. Cold Spring Harbor Laboratory Press, Cold Spring Harbor, NY.
- HOLDEMAN, R., S. NEHRT and S. STROME, 1998 MES-2, a maternal protein essential for viability of the germline in *Caenorhabditis elegans*, is homologous to a *Drosophila* Polycomb group protein. *Development* **125**: 2457–2467.
- HORVITZ, H. R., and J. E. SULSTON, 1980 Isolation and genetic characterization of cell-lineage mutants of the nematode *Caenorhabditis elegans*. *Genetics* **96**: 435–454.
- HSIEH, J., J. LIU, S. A. KOSTAS, C. CHANG, P. W. STERNBERG *et al.*, 1999 The RING finger/B-box factor TAM-1 and a retinoblastoma-like protein LIN-35 modulate context-dependent gene silencing in *Caenorhabditis elegans*. *Genes Dev.* **13**: 2958–2970.
- HUANG, L. S., P. TZOU and P. W. STERNBERG, 1994 The *lin-15* locus encodes two negative regulators of *Caenorhabditis elegans* vulval development. *Mol. Biol. Cell* **5**: 395–412.
- JENUWEIN, T., and C. D. ALLIS, 2001 Translating the histone code. *Science* **293**: 1074–1080.
- KAMATH, R. S., A. G. FRASER, Y. DONG, G. POULIN, R. DURBIN *et al.*, 2003 Systematic functional analysis of the *Caenorhabditis elegans* genome using RNAi. *Nature* **421**: 231–237.
- KAWASAKI, I., Y.-H. SHIM, J. KIRCHNER, J. KAMINKER, W. B. WOOD *et al.*, 1998 PGL-1, a predicted RNA-binding component of germ granules, is essential for fertility in *C. elegans*. *Cell* **94**: 635–645.
- KELLY, W. G., S. XU, M. K. MONTGOMERY and A. FIRE, 1997 Distinct requirements for somatic and germline expression of a generally expressed *Caenorhabditis elegans* gene. *Genetics* **146**: 227–238.
- KEMPKEN, F., and F. WINDHOFER, 2001 The HAT family: a versatile transposon group common to plants, fungi, animals, and man. *Chromosoma* **110**: 1–9.
- KENNEDY, S., D. WANG and G. RUVKUN, 2004 A conserved siRNA-degrading RNase negatively regulates RNA interference in *C. elegans*. *Nature* **427**: 645–649.
- KETTING, R. F., T. H. A. HAVERKAMP, H. G. A. M. VAN LUENEN and R. H. A. PLASTERK, 1999 *mut-7* of *C. elegans*, required for transposon silencing and RNA interference, is a homolog of Werner syndrome helicase and RNaseD. *Cell* **99**: 133–141.
- KIDD, III, A. R., J. A. MISKOWSKI, K. R. SIEGFRIED, H. SAWA and J. KIMBLE, 2005 A β -catenin identified by functional rather than sequence criteria and its role in Wnt/MAPK signaling. *Cell* **121**: 761–772.
- KIM, J. K., H. W. GABEL, R. S. KAMATH, M. TEWARI, A. PASQUINELLI *et al.*, 2005 Functional genomic analysis of RNA interference in *C. elegans*. *Science* **308**: 1164–1167.
- KORENJAK, M., B. TAYLOR-HARDING, U. K. BINNE, J. S. SATTERLEE, O. STEVAUX *et al.*, 2004 Native E2F/RBF complexes contain Myb-interacting proteins and repress transcription of developmentally controlled E2F target genes. *Cell* **119**: 181–193.
- KORF, I., Y. FAN and S. STROME, 1998 The Polycomb group in *Caenorhabditis elegans* and maternal control of germline development. *Development* **125**: 2469–2478.
- LEE, C. C., E. L. BEALL and D. C. RIO, 1998 DNA binding by the KP repressor protein inhibits P-element transposase activity in vitro. *EMBO J.* **17**: 4166–4174.
- LEWIS, P. W., E. L. BEALL, T. C. FLEISCHER, D. GEORLETTE, A. J. LINK *et al.*, 2004 Identification of a *Drosophila* Myb-E2F2/RBF transcriptional repressor complex. *Genes Dev.* **18**: 2929–2940.
- LIPSICK, J. S., 2004 synMuv verite-Myb comes into focus. *Genes Dev.* **18**: 2837–2844.
- LU, X., and H. R. HORVITZ, 1998 *lin-35* and *lin-53*, two genes that antagonize a *C. elegans* Ras pathway, encode proteins similar to Rb and its binding protein RbAp48. *Cell* **95**: 981–991.
- MACFARLAN, T., S. KUTNEY, B. ALTMAN, R. MONTROSS, J. YU *et al.*, 2005 Human THAP7 is a chromatin-associated, histone tail-binding

- protein that represses transcription via recruitment of HDAC3 and nuclear hormone receptor corepressor. *J. Biol. Chem.* **280**: 7346–7358.
- MARCHLER-BAUER, A., J. B. ANDERSON, C. DEWEES-SCOTT, N. D. FEDOROVA, L. Y. GEER *et al.*, 2003 CDD: a curated Entrez database of conserved domain alignments. *Nucleic Acids Res.* **31**: 383–387.
- MARTENS, J. A., and F. WINSTON, 2003 Recent advances in understanding chromatin remodeling by Swi/Snf complexes. *Curr. Opin. Genet. Dev.* **13**: 136–142.
- MELLO, C., and A. FIRE, 1995 DNA transformation, pp. 451–482 in *Caenorhabditis elegans: Modern Biological Analysis of an Organism*, edited by H. F. EPSTEIN and D. C. SHAKES. Academic Press, San Diego.
- MELÉNDEZ, A., and I. GREENWALD, 2000 *Caenorhabditis elegans lin-13*, a member of the LIN-35 Rb class of genes involved in vulval development, encodes a protein with zinc fingers and an LXCXE motif. *Genetics* **155**: 1127–1137.
- MICHEL, K., D. A. O'BROCHTA and P. W. ATKINSON, 2003 The C-terminus of the Hermes transposase contains a protein multimerization domain. *Insect Biochem. Mol. Biol.* **33**: 959–970.
- MISKOWSKI, J., Y. LI and J. KIMBLE, 2001 The *sys-1* gene and sexual dimorphism during gonadogenesis in *Caenorhabditis elegans*. *Dev. Biol.* **230**: 61–73.
- MOGHAL, N., and P. W. STERNBERG, 2003 A component of the transcriptional mediator complex inhibits RAS-dependent vulval fate specification in *C. elegans*. *Development* **130**: 57–69.
- NONET, M. L., O. SAIFEE, H. ZHAO, J. B. RAND and L. WEI, 1998 Synaptic transmission deficits in *Caenorhabditis elegans* synaptobrevin mutants. *J. Neurosci.* **18**: 70–80.
- PARK, E. C., and H. R. HORVITZ, 1986 Mutations with dominant effects on the behavior and morphology of the nematode *Caenorhabditis elegans*. *Genetics* **113**: 821–852.
- PAULSEN, J. E., E. E. CAPOWSKI and S. STROME, 1995 Phenotypic and molecular analysis of *mes-3*, a maternal-effect gene required for proliferation and viability of the germ line in *C. elegans*. *Genetics* **141**: 1383–1398.
- POULIN, G., Y. DONG, A. G. FRASER, N. A. HOPPER and J. AHRINGER, 2005 Chromatin regulation and sumoylation in the inhibition of Ras-induced vulval development in *Caenorhabditis elegans*. *EMBO J.* **24**: 2613–2623.
- REDDY, K. C., and A. M. VILLENEUVE, 2004 *C. elegans* HIM-17 links chromatin modification and competence for initiation of meiotic recombination. *Cell* **118**: 439–452.
- ROSS, J. M., and D. ZARKOWER, 2003 Polycomb group regulation of Hox gene expression in *C. elegans*. *Dev. Cell* **4**: 891–901.
- ROUSSIGNE, M., S. KOSSIDA, A.-C. LAVIGNE, T. CLOUAIRE, V. ECOCHARD *et al.*, 2003 The THAP domain: a novel protein motif with similarity to the DNA-binding domain of *P* element transposase. *Trends Biochem. Sci.* **28**: 66–69.
- RUBIN, E., G. LITHWICK and A. A. LEVY, 2001 Structure and evolution of the hAT transposon superfamily. *Genetics* **158**: 949–957.
- SHIN, T. H., and C. C. MELLO, 2003 Chromatin regulation during *C. elegans* germline development. *Curr. Opin. Genet. Dev.* **13**: 455–462.
- SIEGFRIED, K. R., A. R. KIDD, III, M. A. CHESNEY and J. KIMBLE, 2004 The *sys-1* and *sys-3* genes cooperate with Wnt signaling to establish the proximal-distal axis of the *C. elegans* gonad. *Genetics* **166**: 171–186.
- SIMMER, F., M. TIJSTERMAN, S. PARRISH, S. P. KOUSHIKA, M. L. NONET *et al.*, 2002 Loss of the putative RNA-directed RNA polymerase RRF-3 makes *C. elegans* hypersensitive to RNAi. *Curr. Biol.* **12**: 1317–1319.
- SIMMER, F., C. MOORMAN, A. M. VAN DER LINDEN, E. KUIJK, P. V. E. VAN DEN BERGHE *et al.*, 2003 Genome-wide RNAi of *C. elegans* using the hypersensitive *rrf-3* strain reveals novel gene functions. *PLoS Biol.* **1**: E12.
- SOLARI, F., and J. AHRINGER, 2000 NURD-complex genes antagonise Ras-induced vulval development in *Caenorhabditis elegans*. *Curr. Biol.* **10**: 223–226.
- SULSTON, J. E., and H. R. HORVITZ, 1977 Post-embryonic cell lineages of the nematode, *Caenorhabditis elegans*. *Dev. Biol.* **56**: 110–156.
- TABARA, H., M. SARKISSIAN, W. G. KELLY, J. FLEENOR, A. GRISHOK *et al.*, 1999 The *rde-1* gene, RNA interference, and transposon silencing in *C. elegans*. *Cell* **99**: 123–132.
- THOMAS, J. H., and H. R. HORVITZ, 1999 The *C. elegans* gene *lin-36* acts cell autonomously in the *lin-35 Rb* pathway. *Development* **126**: 3449–3459.
- THOMAS, J. H., C. J. CEOL, H. T. SCHWARTZ and H. R. HORVITZ, 2003 New genes that interact with *lin-35 Rb* to negatively regulate the *let-60 ras* pathway in *Caenorhabditis elegans*. *Genetics* **164**: 135–151.
- TIMMERS, H. T. M., and L. TORA, 2005 SAGA unveiled. *Trends Biochem. Sci.* **30**: 7–10.
- TIMMONS, L., and A. FIRE, 1998 Specific interference by ingested dsRNA. *Nature* **395**: 854.
- UNHAVAITHAYA, Y., T. H. SHIN, N. MILIARAS, J. LEE, T. OYAMA *et al.*, 2002 MEP-1 and a homolog of the NURD complex component Mi-2 act together to maintain germline-soma distinctions in *C. elegans*. *Cell* **111**: 991–1002.
- VON ZELEWSKY, T., F. PALLADINO, K. BRUNSCHWIG, H. TOBLER, A. HAJNAL *et al.*, 2000 The *C. elegans* Mi-2 chromatin-remodelling proteins function in vulval cell fate determination. *Development* **127**: 5277–5284.
- WALKER, D. S., S. LY, N. J. D. GOWER and H. A. BAYLIS, 2004 IRI-1, a LIN-15B homologue, interacts with inositol-1,4,5-triphosphate receptors and regulates gonadogenesis, defecation, and pharyngeal pumping in *Caenorhabditis elegans*. *Mol. Biol. Cell* **15**: 3073–3082.
- WANG, D., S. KENNEDY, D. CONTE, JR., J. K. KIM, H. W. GABEL *et al.*, 2005 Somatic misexpression of germline P granules and enhanced RNA interference in retinoblastoma pathway mutants. *Nature* **436**: 593–597.
- XU, L., J. PAULSEN, Y. YOO, E. B. GOODWIN and S. STROME, 2001 *Caenorhabditis elegans* MES-3 is a target of GLD-1 and functions epigenetically in germline development. *Genetics* **159**: 1007–1017.
- XUE, Y., R. GIBBONS, Z. YAN, D. YANG, T. L. McDOWELL *et al.*, 2003 The ATRX syndrome protein forms a chromatin-remodeling complex with Daxx and localizes in promyelocytic leukemia nuclear bodies. *Proc. Natl. Acad. Sci. USA* **100**: 10635–10640.
- ZHOU, L., R. MITRA, P. W. ATKINSON, A. B. HICKMAN, F. DYDA *et al.*, 2004 Transposition of *hAT* elements links transposable elements and V(D)J recombination. *Nature* **432**: 995–1001.

Communicating editor: A. VILLENEUVE